1984-12

Noise characteristics of an avalanche photodiode

Kim, Eun Gi

Monterey, California. Naval Postgraduate School

NAVAL POSTGRADUATE SCHOOL
Monterey, California

THESIS

NOISE CHARACTERISTICS
OF
AN AVALANCHE PHOTODIODE

by

Eun Gi Kim
December 1984

Thesis Advisor E. L. Walters

Approved for public release; distribution unlimited.

REPORT DOCUMENTATION PAGE

READ INSTRUCTIONS BEFORE COMPLETING FORM

1. REPORT NUMBER
2. GOVT ACCESSION NO.
3. RECIPIENT'S CATALOG NUMBER

4. TITLE (and Subtitle)
Noise Characteristics of an Avalanche Photodiode

5. TYPE OF REPORT & PERIOD COVERED
Master's Thesis
December 1984

6. PERFORMING ORG. REPORT NUMBER

7. AUTHOR(s)
Eun Gi Kim

8. CONTRACT OR GRANT NUMBER(s)

9. PERFORMING ORGANIZATION NAME AND ADDRESS
Naval Postgraduate School
Monterey, California 93943

10. PROGRAM ELEMENT, PROJECT, TASK AREA & WORK UNIT NUMBERS

11. CONTROLLING OFFICE NAME AND ADDRESS
Naval Postgraduate School
Monterey, California 93943

12. REPORT DATE
December 1984

13. NUMBER OF PAGES
45

14. MONITORING AGENCY NAME & ADDRESS(if different from Controlling Office)

15. SECURITY CLASS. (of this report)
Unclassified

15a. DECLASSIFICATION/DOWNGRADING SCHEDULE

16. DISTRIBUTION STATEMENT (of this Report)
Approved for public release; distribution unlimited

17. DISTRIBUTION STATEMENT (of the abstract entered in Block 20, if different from Report)

18. SUPPLEMENTARY NOTES

19. KEY WORDS (Continue on reverse side if necessary and identify by block number)
Avalanche Photodiode

20. ABSTRACT (Continue on reverse side if necessary and identify by block number)
The responsivity, noise equivalent power, specific detectivity, shot noise and multiplication noise of a RCA C30872 silicon reach-through avalanche photodiode were studied at 4 wavelengths 563.8 nm, 569.9 nm, 699.6 nm, and 826.2 nm. The detector noise was resolved into amplifier, shot and a multiplied
(continued)

Item 20. (continued)

leakage components as a function of the reverse bias voltage. Experimental results are discussed and it is concluded that this photodiode has an optimum reverse bias voltage of about 250 volts that maximizes the specific detectivity and minimizes the noise equivalent power. The avalanche photodiode excess noise factor was found to be 1.4-2.0 at low gain and increase to 9.17 at a gain of 440.

Approved for public release; distribution is unlimited.

Noise Characteristics of an Avalanche Photodiode

by

Eun Gi Kim
Major, Republic of Korea Air Force
B.S., Republic of Korea Air Force Academy

Submitted in partial fulfillment of the
requirements for the degree of

MASTER OF SCIENCE IN PHYSICS

from the

NAVAL POSTGRADUATE SCHOOL
December 1984

ABSTRACT

The responsivity, noise equivalent power, specific detectivity, shot noise and multiplication noise of a RCA C30872 silicon reach-through avalanche photodiode were studied at 4 wavelengths 563.8 nm, 569.9 nm, 699.6 nm, and 826.2 nm. The detector noise was resolved into amplifier, shot and a multiplied leakage components as a function of the reverse bias voltage. Experimental results are discussed and it is concluded that this photodiode has an optimum reverse bias voltage of about 250 volts that maximizes the specific detectivity and minimizes the noise equivalent power. The avalanche photodiode excess noise factor was found to be 1.4-2.0 at low gain and increases to 9.17 at a gain of 440.

TABLE OF CONTENTS

LIST OF TABLES

LIST OF FIGURES

ACKNOWLEDGEMENT

At this time I would like to express my appreciation to the many people who have offered generously of their time and experience. Without their generosity, the completion of this project would have been more difficult.

The experience and technical assistance of Mr. R. Moeller proved crucial in the calibration of LEDs and Si-RAPD.

The advice and support of professor E. A. Milne was always welcome. My thanks to professor D. L. Walters for his patient, ever present guidance and direction.

I. INTRODUCTION

Silicon reach-through avalanche photodiodes (hereafter, abbreviated RAPD) provide low noise, high quantum efficiency and fast response characteristics when used as optical detectors. Conventional silicon photodiodes do not provide gain, consequently detection systems using these diodes are frequently amplifier noise limited. Avalanche photodiodes can provide gain, on the order of 10-1000, that can overcome this amplifier noise. This additional gain can be beneficial for amplifier noise limited situations, however, the gain comes at the expense of excess noise that is inherent with the ionization-multiplication process. The RCA C30872 RAPD is a state-of-the-art silicon avalanche photodiode that has potential applications in laser detection and range finding as well as atmospheric remote sensors.

The noise and responsivity characteristics of this RCA RAPD are needed in order to perform systems design calculations comparing this detector with other detectors such as photomultipliers.

II. THEORETICAL CONSIDERATIONS

A. RAPD STRUCTURE AND CHARACTERISTICS

The standard RAPD is shown in Figure 2.1. The pn junction has a long depletion region that is separated into a wide drift region and a narrow multiplying region. Photons are absorbed in the drift region, while photogenerated carriers cause impact ionization in the multiplying region. As the reverse bias across this diode increases, the depletion layer widens into the lighter doped p-region. The total number of impurity atoms contained in the p-region is such that the field there causes some avalanche multiplication at a reach-through voltage for which the depletion

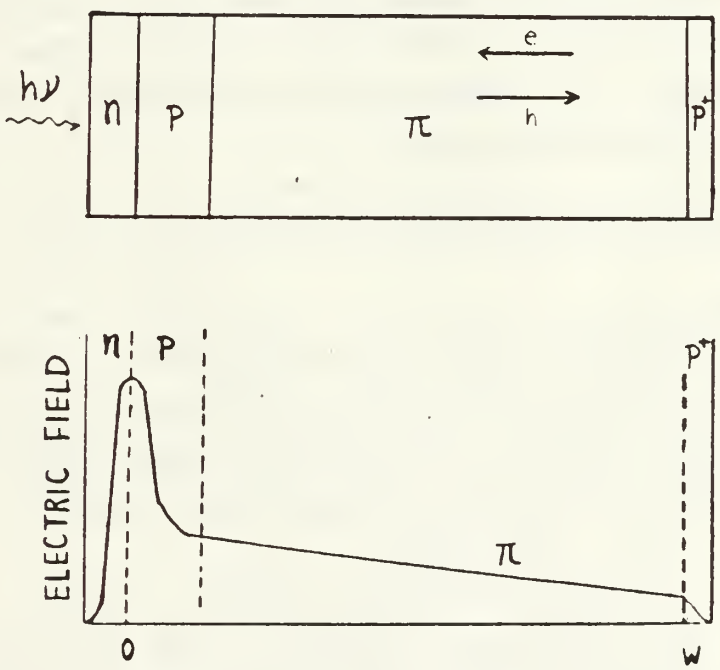

Figure 2.1 Standard RAPD Structure.

layer reaches through to the intrinsic region. Increasing the voltage beyond this point causes the depletion layer to advance to the p contact without greatly changing the field amplitude in the rest of device. The result is a gradual variation of gain with reverse bias voltage and improved noise figure [Ref. 1]. This structure has some distinct advantages over other structures from the point of view of studying the avalanche processes in the diode. The RAPD combines the excellent frequency response of a PIN diode [Ref. 2] with a highly stable current gain achieved by avalanche multiplication of photogenerated carriers. Gain through avalanche multiplication has been reported for pn diodes [Ref. 3] as well as PIN photodiodes [Ref. 4]. The high frequency response of pn diodes is limited by carrier diffusion times and by a relatively large junction capacitance. For both diode types, it is difficult to achieve a stable high gain because of the rapid increase of the multiplication factor as the reverse bias voltage nears breakdown. The RAPD has been designed in such a way as to minimize these problems.

B. THEORY OF MULTIPLICATION NOISE IN RAPD

The total noise for a Si-RAPD amplifier system is composed of shot noise, multiplication noise and equivalent amplifier noise. Shot noise is caused by the discrete nature of electron flow. Associated with the averaged primary photocurrent is a mean square shot noise,

$$\langle i_s^2 \rangle = 2eI_{d1}\,\Delta f, \qquad (2\text{-}1)$$

where e is the electronic charge, I_{d1} is the photocurrent that is not multiplied and Δf is the electronic signal bandwidth. When no avalanche multiplication takes place, the Si-RAPD dark current induces a shot noise given by equation (2-1). Dark current is the current that flows through the

photodiode in the absence of light. Part of this current is caused by leakage current flowing through the junction edges. Another part of the dark current comes from the space-charge current generated in the depletion layer such that the carriers are swept into the multiplying region, undergoing gain. This current is one or two orders of magnitude less than the pn junction edge current. For convenience, equivalent amplifier noise is defined as the sum of all possible noise - preamplifier noise, power supply noise, etc. - that exists in the noise measuring system excluding the shot noise and multiplication noise, and is not a function of gain. Multiplication noise (or excess noise) is generated by the photocarriers--electrons and holes--impact ionization process [Ref. 5]. The mean square excess noise in the amplified current can be written in the form

$$\langle i_m^2 \rangle = 2eI_{d_2} M^2 F \Delta f = 2eI_{eq} \Delta f, \qquad (2\text{-}2)$$

where e is the electron charge, M is the gain (M=1 in the case of a nonmultiplying photodiode), F is the excess noise factor and Δf is the noise bandwidth. I_{d_2} is that component of the dark current that undergoes multiplication, I_{eq} is the equivalent dark current defined by $I_{eq} = I_{d_2} M^2 F$ and M(x) is the position dependent multiplication factor introduced by McIntyre [Ref. 6]

$$M(x) = \frac{\exp\left\{-\int_o^W [\alpha(x') - \beta(x')]dx'\right\}}{1 - \int_o^W \alpha(x) \exp\left\{-[\alpha(x') - \beta(x')]dx'\right\}dx} . \qquad (2\text{-}3)$$

F is the ratio of the actual noise to that which would exist if the avalanche process were noiseless. An expression for the excess noise factor F is given by [Ref. 6], [Ref. 7].

$$F = M\left[1-(1-k)(M-1)^2/M^2\right], \qquad (2\text{-}4)$$

where k is the ratio of electron-to-hole ionization coeffcients α/β under the assumtion that α/β is independent of electric field. When the electric field dependence of α/β is included, k may be replaced by an effective value k_{eff} [Ref. 6], [Ref. 7]. From equation (2-4) we see that minimum

noise occurs for small k (high hole ionization). For silicon, in the electric field range of interest (2 to 4×10^5 v/cm) k is expected to be approximately 0.05 to 0.1 [Ref. 8].

The dominant noise source in RAPD is multiplication noise. In the avalanche process, both signal and noise are amplified. In addition, a noise due to fluctuations in the impact ionization rate occurs. Therefore the multiplication noise must be a fuction of the gain. McIntyre [Ref. 9] has shown that the total noise current $\langle i_n^2 \rangle$ in the case where electrons are the predominant ionizing carrier is

$$\langle i_n^2 \rangle = \langle i_s^2 \rangle + \langle i_m^2 \rangle + \langle i_a^2 \rangle, \qquad (2\text{-}5)$$

where $\langle i_s^2 \rangle$ is the mean square shot noise, $\langle i_m^2 \rangle$ is the mean square multiplication noise and $\langle i_a^2 \rangle$ is an equivalent pre-amplifier noise current.

III. EXPERIMENTAL ARRANGEMENT

A. GENERAL

The responsivity and noise characteristics of the RCA Si-RAPD were investigated using four modulated LEDs as light sources. In order to use the LEDs as light sources the radiant flux versus input current and the spectral distribution of the light from each diode needed to be measured. The emitted light intensity at each LED wavelength was measured using a calibrated silicon PIN photodiode (United Detector Technology Model PIN-10DP, Serial #797). The current from the PIN diode over the 10^{-12} to 10^{-4} ampère range was measured with a Keithley 600B electrometer. The input current to the LEDs was in the 10^{-6} to 10^{-3} ampère range.

Initially the LEDs(Light Emitting Diodes) were placed adjacent to the large area (41.2 mm^2) calibrated, silicon PIN diode in order to collect virtually all of the emitted light. This configuration provided the maximum dynamic range in the PIN output currents. Since the angular distribution of energy from the LEDs was nonuniform, the solid angles of the LED's were reduced by using a 10 cm long tube that had three 0.49 cm baffles. The truncated light cone (2.8 degrees) from the diodes produced a smaller solid angle that had a relatively uniform light distribution.

After verifying that the light intensity was uniform across the 0.49 cm exit aperture of the light baffle tube, the calibrated PIN photodiode and Keithley 600B electrometer were again used to measure the truncated LED light flux versus LED input current. The two PIN output current versus LED input current curves, one without the tube and one with the tube, were identical for a given LED current except for

the solid angle reduction factor. This allowed us to calibrate the restricted solid angle LED flux over a factor of 100-200 larger dynamic range than our Keithley 600B electrometer could measure directly.

The spectral distribution of each LED was measured with a prism spectrometer (BECKMAN DK-1A). After the raw spectra were corrected for the spectrometer instrument response, the centroid wavelength was used in conjuction with the silicon PIN photodetector responsivity calibration table to arrive at an absolute calibration of the emitted light from each LED.

The shot noise and excess noise from an avalanche photodiode depend on the reverse bias leakage current. This current was measured as a function of the reverse bias voltage by measuring the voltage drop of this current across a 10^6 ohm resistor amplified by a PAR 113 pre-amplifier.

The noise, gain and responsivity of the Si-RAPD were all measured by using the 10 cm solid angle reducing tube and modulating the LEDs with a 10 Hz positive square wave current. The Si-RAPD response to this signal was measured with a HP 3561A FFT spectrum analyzer after being amplified by a PAR 113 high-gain, low-noise pre-amplifier. The signal analyzer allowed us to seperate the modulated signal from the broadband noise and residual 60 Hz noise. The magnitude of the unipolar current driving the LED was measured with the Keithley 600B electrometer at 0.1 Hz. The light flux on the Si-RAPD was derived from the calibrated LED light output versus input current measurements after correcting for the known responsivity of the calibrated PIN photodiode at the LED emitting wavelength and the effective area of the Si-RAPD.

B. DETAILS OF EXPERIMENT

1. LED Intensity Profile

In order to produce a uniform intensity profile from the LED's, the angular distribution was restricted. A 10 cm long tube with 3 baffles each with a 0.49 cm diameter hole restricted the cone angle of the LED radiation to about 2.8 degrees. This tube is shown in Figure 3.1. The uniformity of the truncated intensity profile was measured by scanning the exit field of the solid angle reducing tube with a photomultiplier masked by a 0.05 mm pin hole. As shown in Figure 3.2, the angular distribution of the energy across the exit aperture was uniform to within 1-2 %.

Since the PIN and Si-RAPD photodetectors were mounted a slight distance behind the exit aperture of the solid angle reducing tube, the divergence angle of the column of light leaving the tube was measured as shown in Figure 3.3. The divergence angle was found to be 0.29 degrees between 0.1 cm and 7.1 cm behind the exit aperture.

The PIN currents were measured with a Keithley 600B electrometer that had a lower current limit of about 10 amperes. To obtain a wider dynamic range of measurable currents, the PIN currents were measured with the LED adjacent to the PIN photodiode. A second set of measurements with the tube between the LED and the PIN photodetector were also collected. The results are shown in Figures 3.4 - 3.7. The solid curves are cubic spline interpolation fits to the data. The two curves in the figures are identical to each other to within a multiplicative constant except at the lowest current levels where errors in the electrometer became significant.

The proportionality constants between the detected PIN currents with and without the tube are shown in Table 1 along with the LED peak and centroid wavelengths.

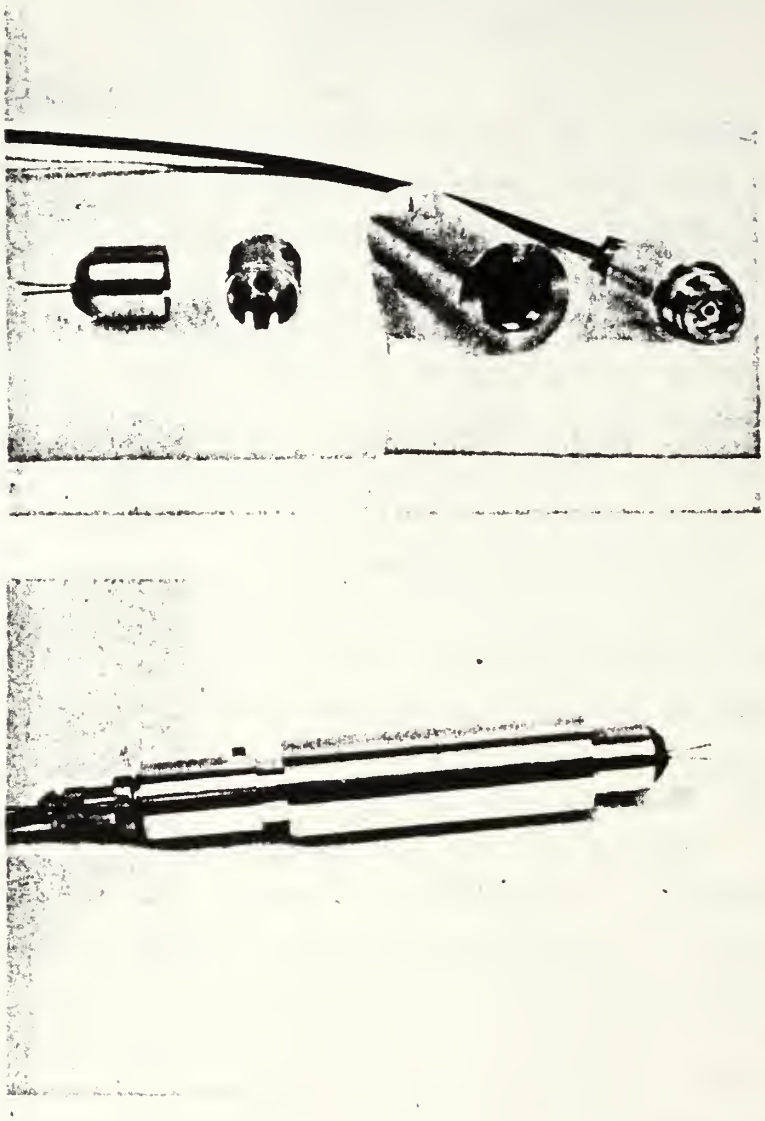

Figure 3.1 Solid Angle Reducing Tube with Antireflection Baffles, Caliblated LED and Si-RAPD.

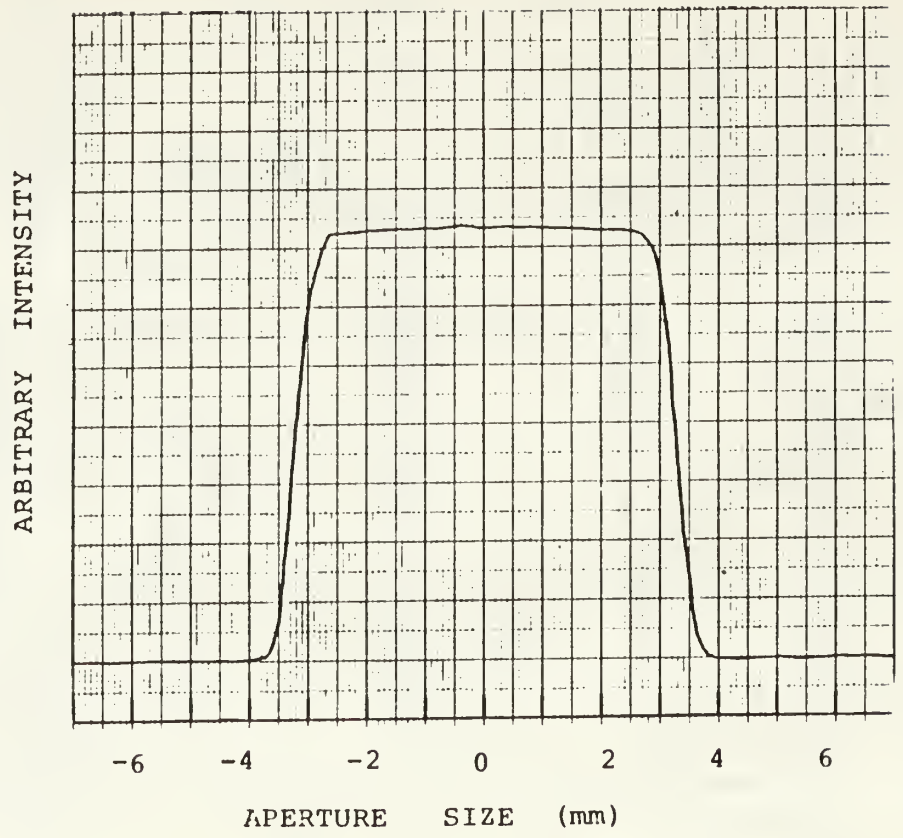

Figure 3.2 Uniformity of the LED Radiation Emerging from the Solid Angle Reducing Tube.

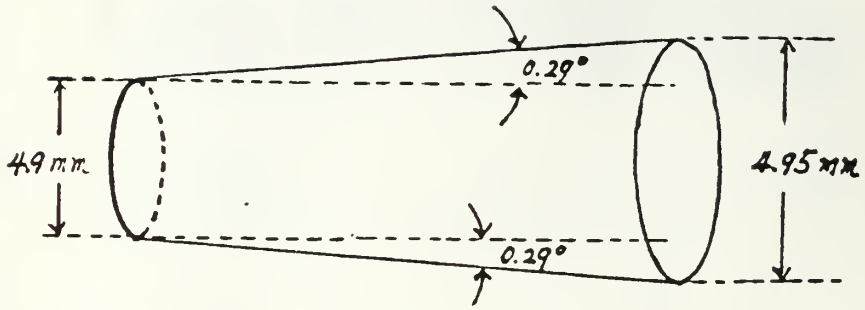

Figure 3.3 Divergence Angle between 0.1 cm and 7.1 cm behind the Exit Aperture.

TABLE 1

LED Emission Characteristics

LED	peak wavelength	centroid	solid angle reduction factor
#1	558 nm	563.8 nm	280.83
#2	563.5 nm	569.9 nm	146.41
#3	680.6 nm	699.6 nm	286.79
#4	820.4 nm	826.2 nm	71.94

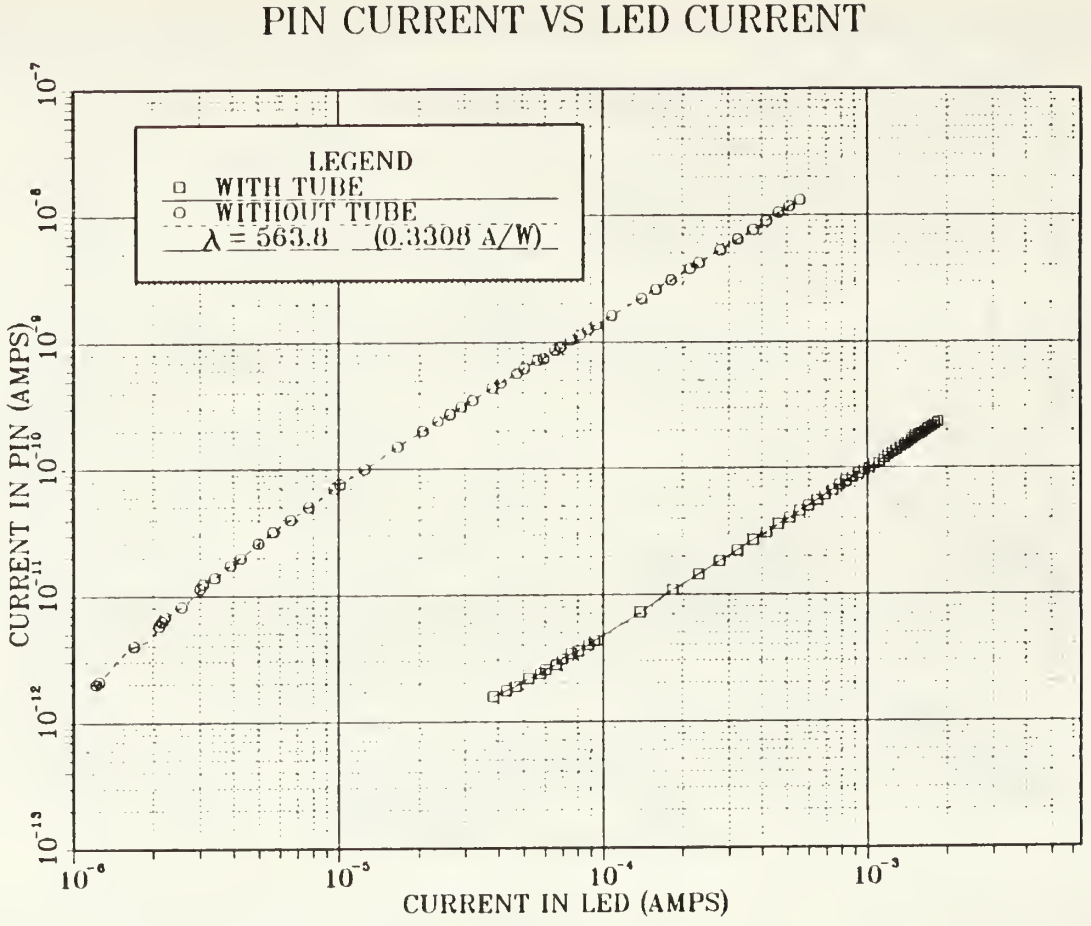

Figure 3.4 Detected PIN Photocurrent vs the LED Drive Current with and without the Solid Angle Reduction: 0.3308 A/W at 563.8 nm.

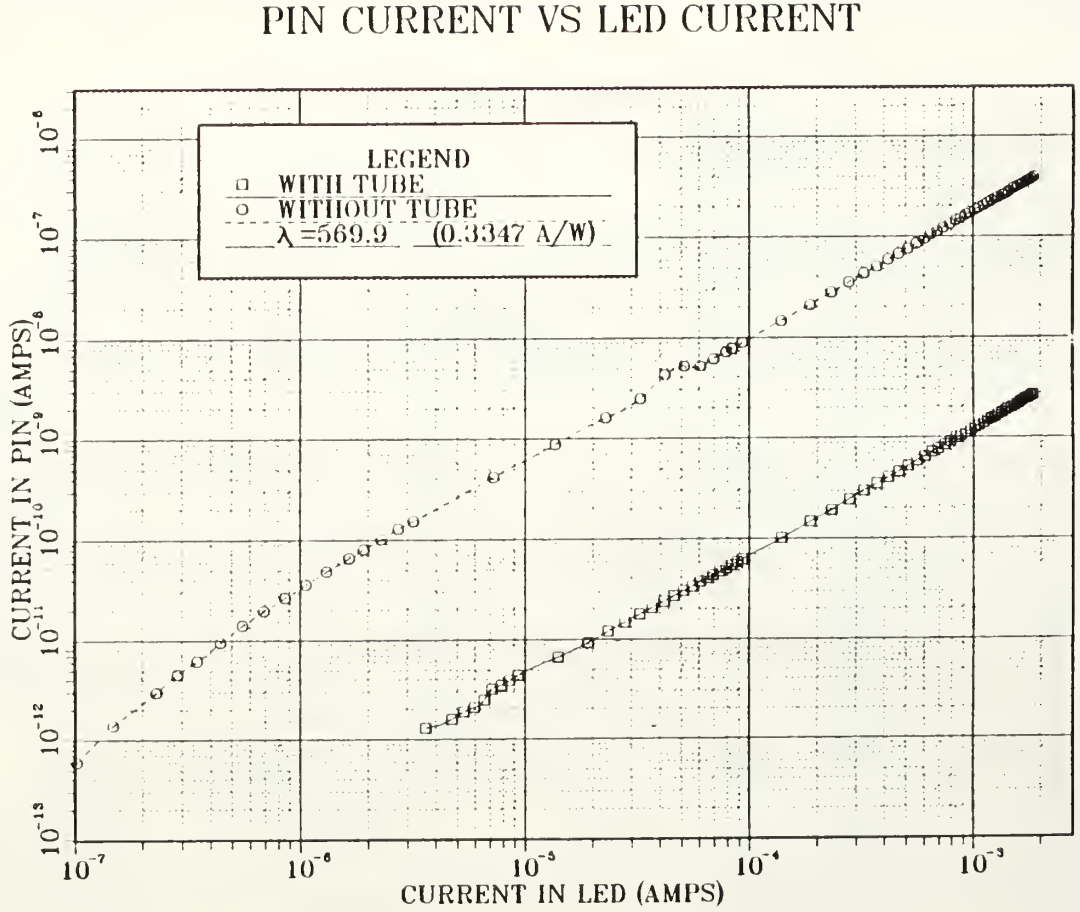

Figure 3.5 Detected PIN Photocurrent vs the LED Drive Current with and without the Solid Angle Reduction: 0.3347 A/W at 569.9 nm.

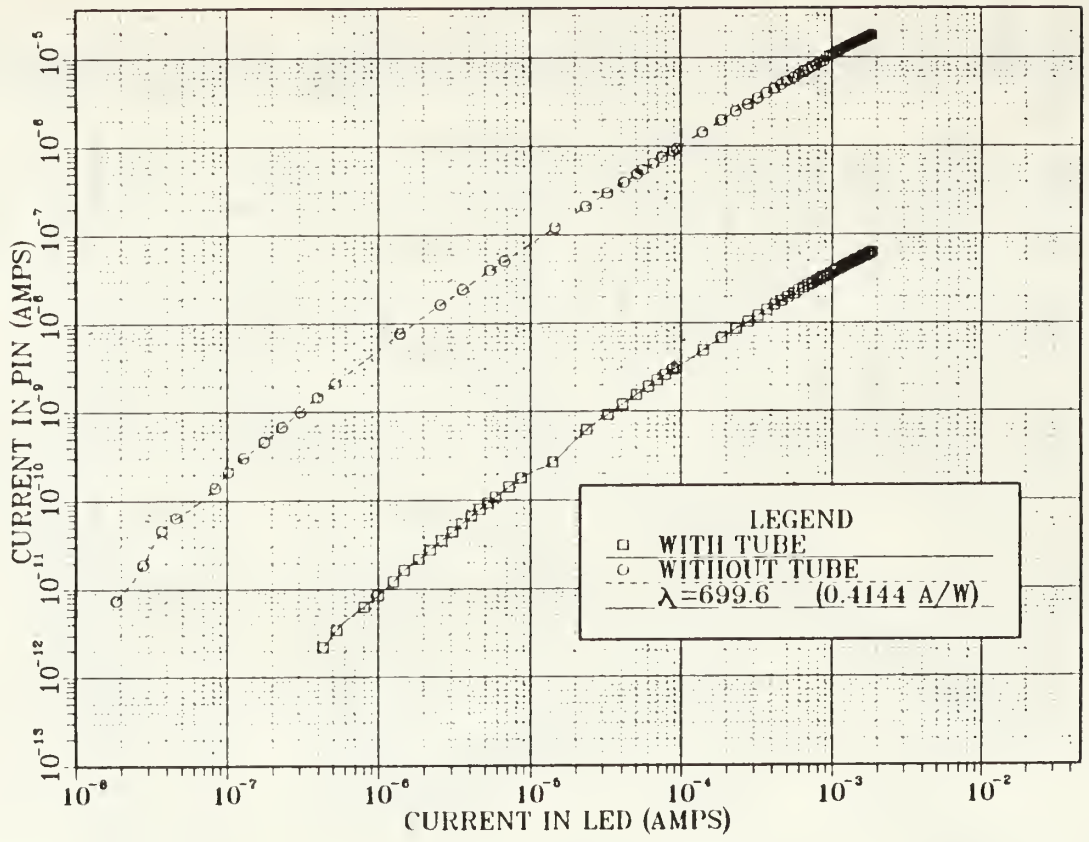

Figure 3.6 Detected PIN Photocurrent vs the LED Drive Current with and without the Solid Angle Reduction: 0.4144 A/W at 699.6 nm.

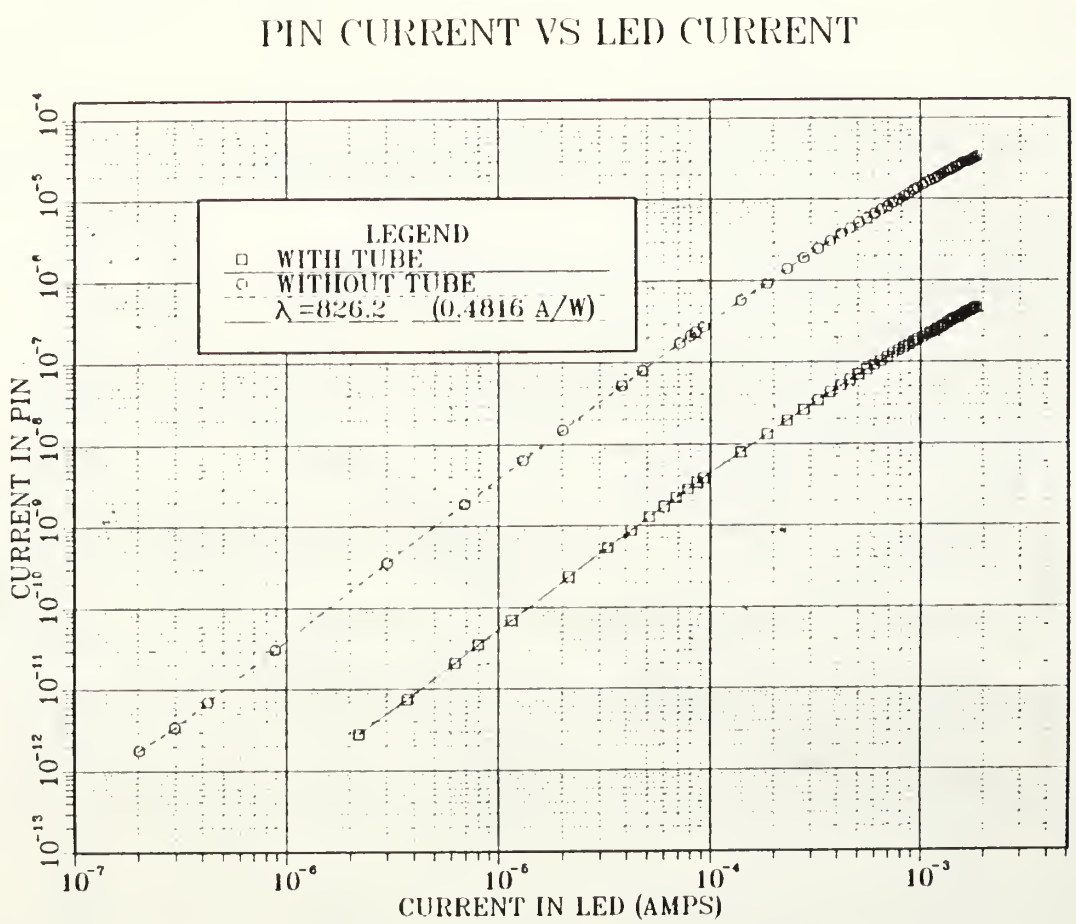

Figure 3.7 Detected PIN Photocurrent vs the LED Drive Current with and without the Solid Angle Reduction: 0.4816 A/W at 826.2 nm.

2. Spectral Response of the LED Emission

The spectral distribution of the LED emitted radiation was measured with a BECKMAN DK-1A Recording Spectrometer. This prism spectrometer used a RCA 4840 photomultiplier that has a responsivity that decreases rapidly for wavelengths longer than 700 nm. In order to obtain the correct LED emission profile it was necessary to divide the raw measurements by the spectrometer intensity response versus wavelength. The spectra of #1 LED and #4 led are shown in Figures 3.8-3.9. The spectral shift amounts to about 5 nm for the 820 nm LED. Figures 3.8-3.9 show that the peak wavelength of #1 LED does not change but that of #4 LED does. The centroid of the corrected LED emission profiles were calculated numerically using a Simpson's rule algorithm [Ref. 10]. Significantly, the peak emission wavelength and the centroid are different for each diode as seen in Table 1.

The LED irradiance was derived from Figures 3.4-3.7 by dividing the PIN output current by the responsivity of the PIN photodetector at the LED centroid wavelengths.

3. Noise Measurements

The reverse bias current was measured as a function of the bias voltage by measuring the voltage drop of this current across a 10^6 ohm resistor amplified by a PAR 113 pre-amplifer with no light incident on the Si-RAPD. The circuit diagram for obtaining the noise, gain and some properties of Si-RAPD is shown in Figure 3.10.

Initially, a 1N914 Si-pn diode was connected in parallel with the 10^6 ohms resistor to prevent damage to the PAR 113 pre-amplifier should the Si-RAPD reach breakdown. This produced a problem in the initial data reduction when the responsivity of the Si-RAPD appeared to be a factor of

two below the manufacture's specifications. The 1N914 was the problem since it had a shunt resistance of 10^6 ohms or lower above 0.1 volt forward bias.

A HP 6236B Power Supply provided the positive bias voltage to the Si-RAPD. As the applied voltage across the photodiode increased, the measured diode noise increased. The light signal through the 10 cm long tube from the LED to the Si-RAPD was modulated with a 10 Hz positive square wave from a HP 3314 Function Generator. The detected signal and noise were amplifed by a PAR 113 pre-amplifier. The HP 3461A spectrum analyzer allowed us to seperate the modulated signal from the broadband noise and any 60 Hz residual noise. A typical spectrum from this signal analyzer is shown in Figure 3.11. The scanning range was from 0 Hz to 100 Hz, one thousand individual spectra were averaged in order to reduce the variation in the noise spectra.

4. Responsivity of the Si-RAPD

The responsivity of the Si-RAPD was derived from the HP 3431A spectrum analyzer using the following equations

$$\begin{aligned} P_1 &= i_p / R_p, \\ P_2 &= P_1 \times AR, \\ R_o &= [(2 \times i_R) / f] / P, \\ R &= R \times M, \end{aligned} \qquad (3\text{-}1)$$

where P_1 is the power of PIN phodiode at 10 cm from LED, i_p is the current in the PIN diode, R_p is the PIN responsivity at 10 cm, P_2 is the incident power on the Si-RAPD using the tube, AR is the ratio between the area of the exit aperture and the effective area of the Si-RAPD, i_R is the current in the Si-RAPD and R_o is the responsivity at gain 1. The factor of 2 in the third row in equation (3-1) means upper and lower part of sine wave, f is the fundamental frequency sine wave amplitude for a given square wave input amplitude $(4/\pi)$ and M is the gain. The experimental results will be discussed in the next chapter.

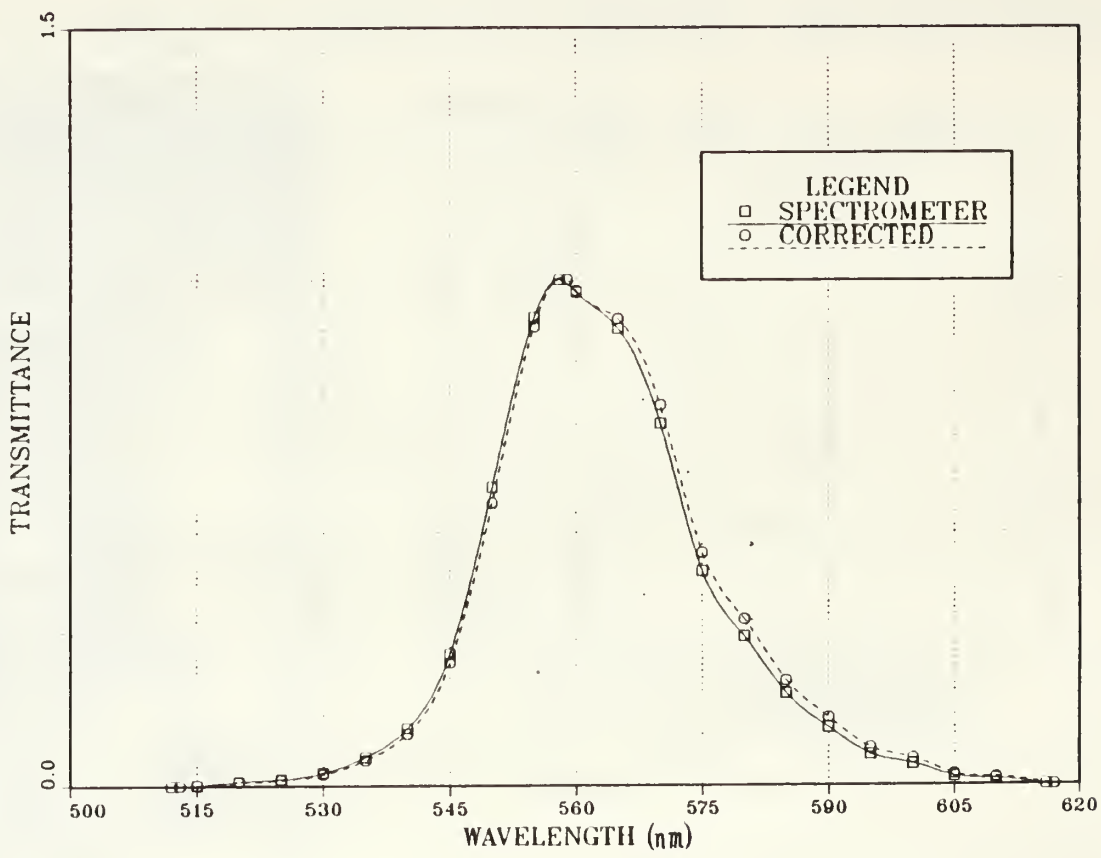

Figure 3.8 Emission Spectrum of #1 LED before and after Correcting for the Spectrometer Sensitivity Variations with Wavelength.

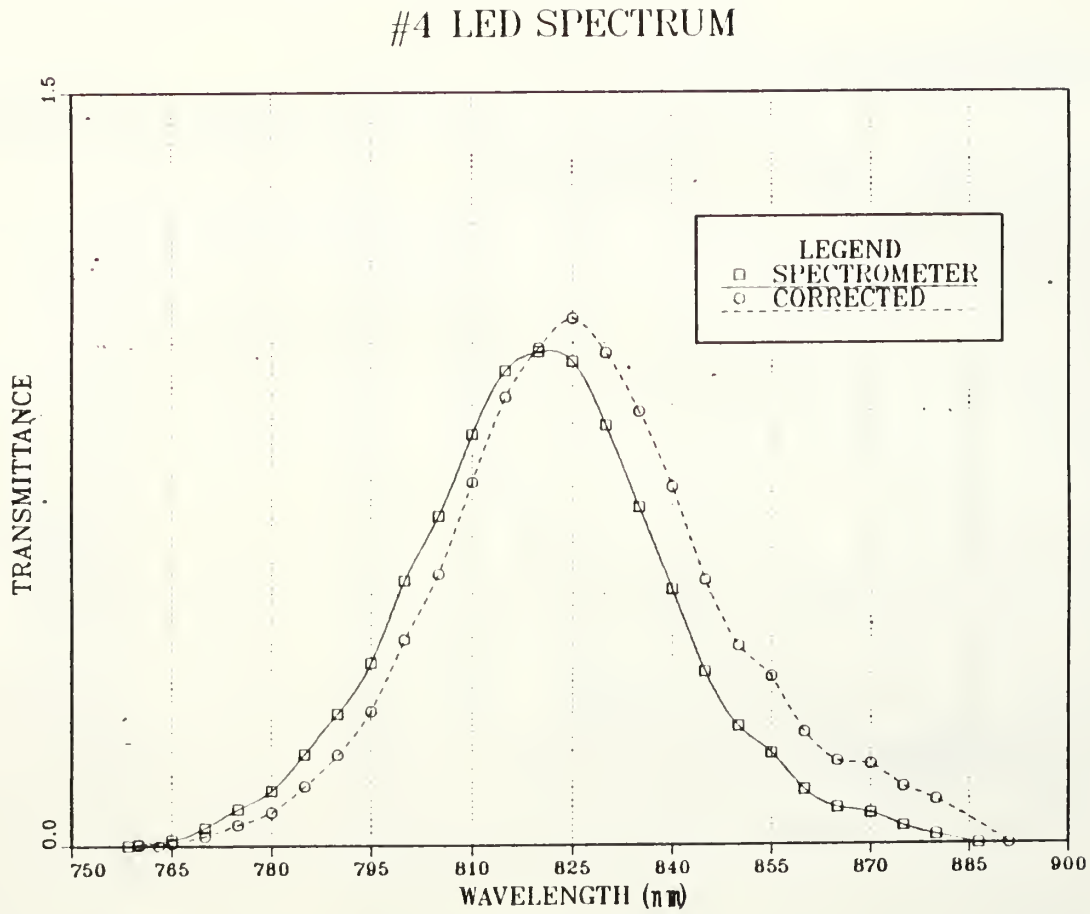

Figure 3.9 Emission Spectrum of #4 LED before and after Correcting for the Spectrometer Sensitivity Variations with Wavelength.

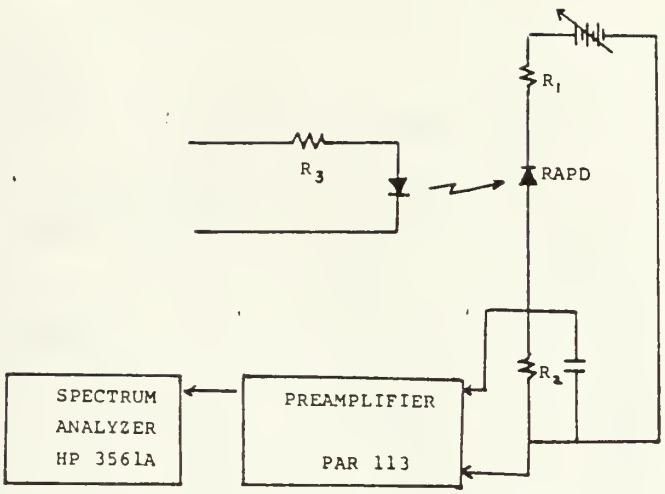

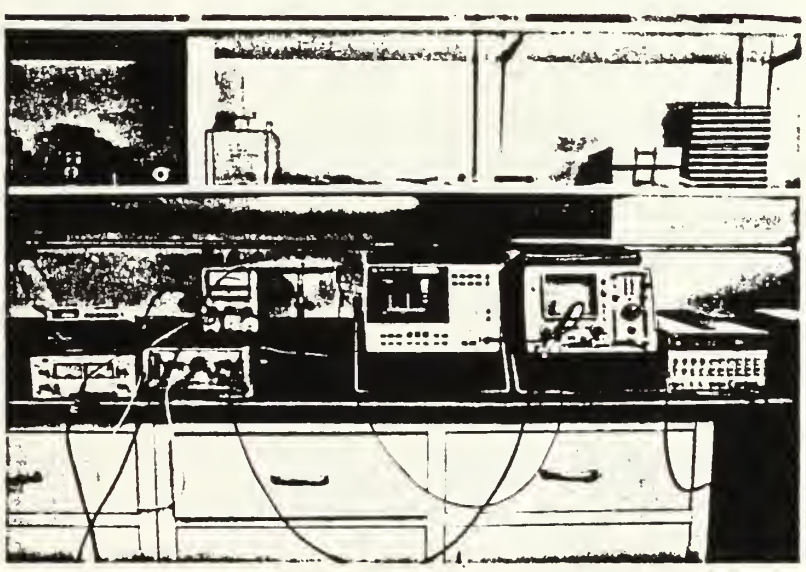

Figure 3.10 Schematic Arrangement for Measuring Noise.

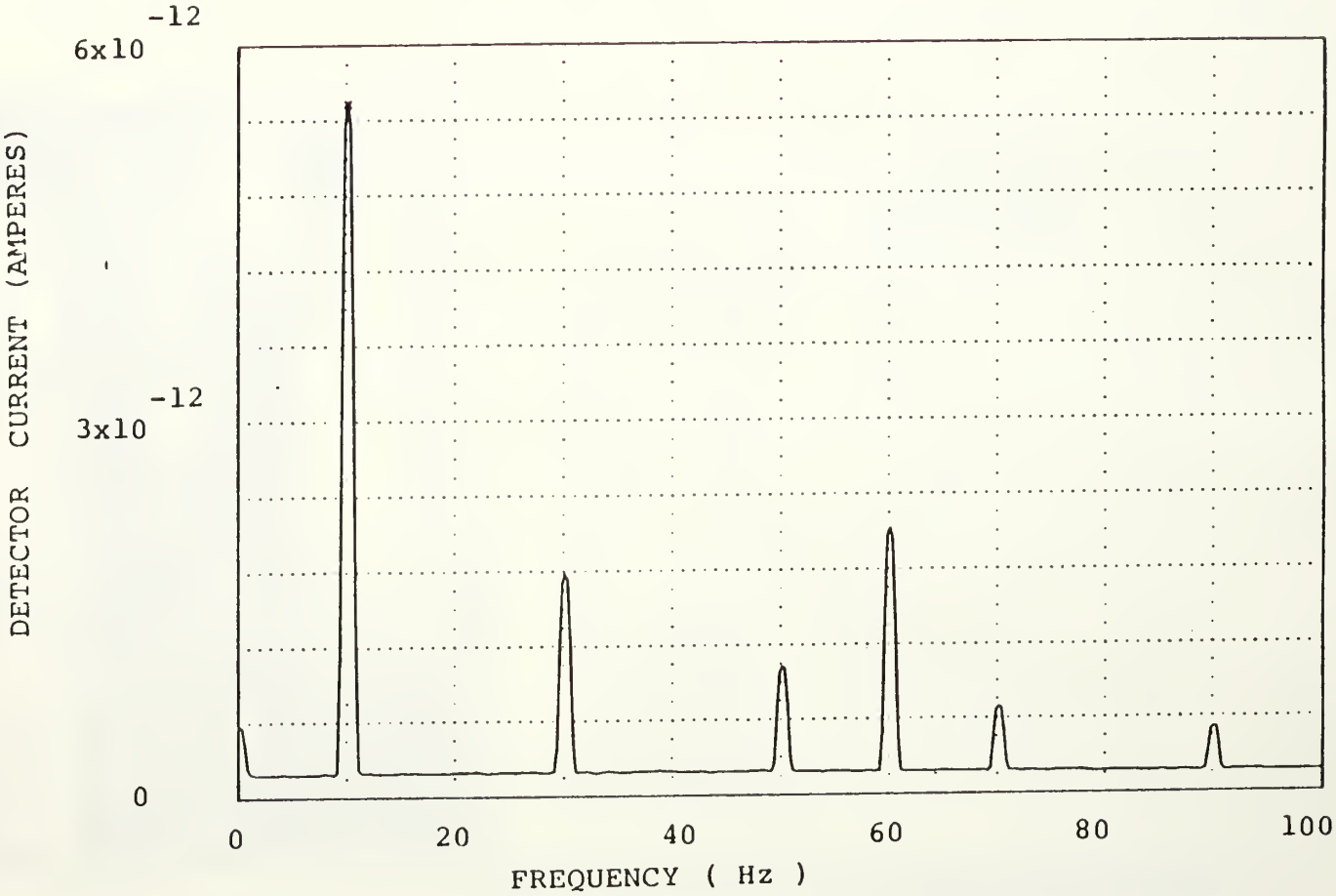

Figure 3.11 Typical Hp 3431A Signal and Noise Spectra: 10 Hz Square Wave First Harmonic, Residual 60 Hz Noise, 1000 Averaged Noise Spectra at a Reverse Bias Voltage of 100 Volts.

IV. EXPERIMENTAL RESULTS

The main experimental results of the noise and responsivity measurements are discussed below.

A. SHOT NOISE

When no multiplication takes place, the shot noise arries from the Si-RAPD dark current. Figure 4.1 shows the measured dark current as a function of the reverse bias voltage with no incident light. The dark current shows a slight increase at bias voltages between 120 volts and 130 volts. This abrupt increase indicates that the electron field in the multiplication region of Figure 2-1 has become large enough to initiate the avalanche gain process. Futhermore, from theory we know that the dark current includes two components: a leakage component and a multiplied component which flows through the junction. The noise currents induced by these two dark currents are shown in the upper curve of Figure 4.2. The lower curve is the shot noise computed from the reverse bias leakage current using equation (2-1). The difference between the actual noise and the shot noise at zero bias voltage is the equivalent amplifier noise as defined in chapter 2. The magnitude of the equivalent amplifier noise current is 5×10^{-12} amps/hz .

Figure 4.3 shows the photocurrent multiplication factor (or gain) M as a funtion of the dark current. It is the evident that reach-through occurs around a bias voltage of 120-130 volts. Beyond this point, additional applied voltage gradually increases the field and hence the gain.

On a log-log plot the dark current plotted versus gain has a linear relation when the gain is greater than 70, as

shown in Figure 4.4. The linear portion of the dark current is extrapolated to M=1. Its intersection with the vertical axis corresponds to the dark current component I_{d2} in equation (2-2), which is multiplied in the avalanche process. The surface leakage current component is equal to the difference between the total dark current at low gains and the dark component I_{d2}. The dark current component subject to multiplication I_{d2} is less than 10^{-11} amps at room temperature and the multiplication noise factor is proportional to $M^{2.326}$.

B. EXCESS NOISE FACTOR

The effective ionization coefficient ratio, K_{eff}, equation (2-4), obtained from these experimental results is 0.0154 ± 0.0124 for a RCA C30872 Si-RAPD. The excess noise factor F versus gain M for k_{eff} = 0.0154 is plotted in Figure 4.5 .

C. RESPONSIVITY OF THE SI-RAPD

The responsivity of a detector is the output current or voltage produced per unit input power. Figure 4.6 shows the wavelength versus responsivity (in ampères/watts) as a funtion of gain. As expected the responsivity increases as the wavelength increases since we are approaching the silicon band gap energy and the photons can penetrate to the vicinity of the depletion region. The effective area of the photodiodes is somewhat less than the nominal 0.7mm due to electrostatic edge effects. This tends to reduce the peak field in the avalanche region near the edge reducing the responsivity.

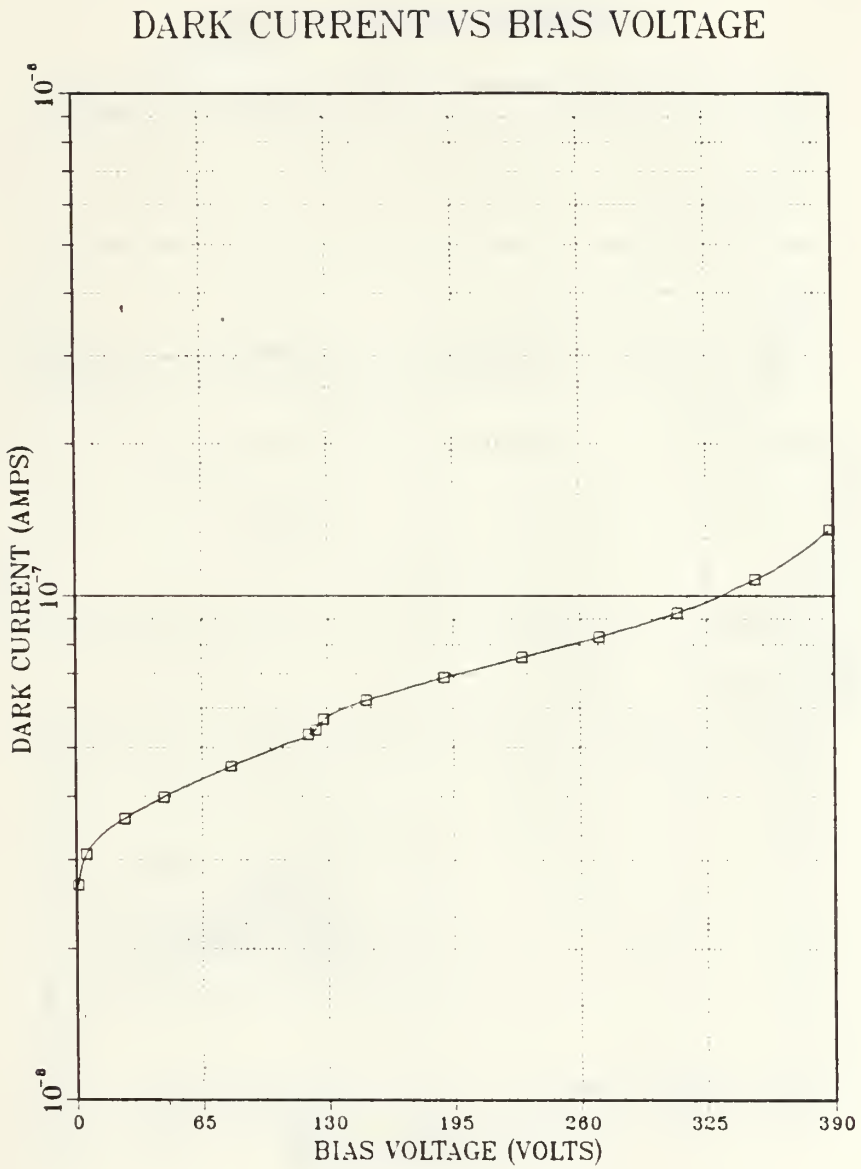

Figure 4.1 Dark Current versus Bias Voltage.

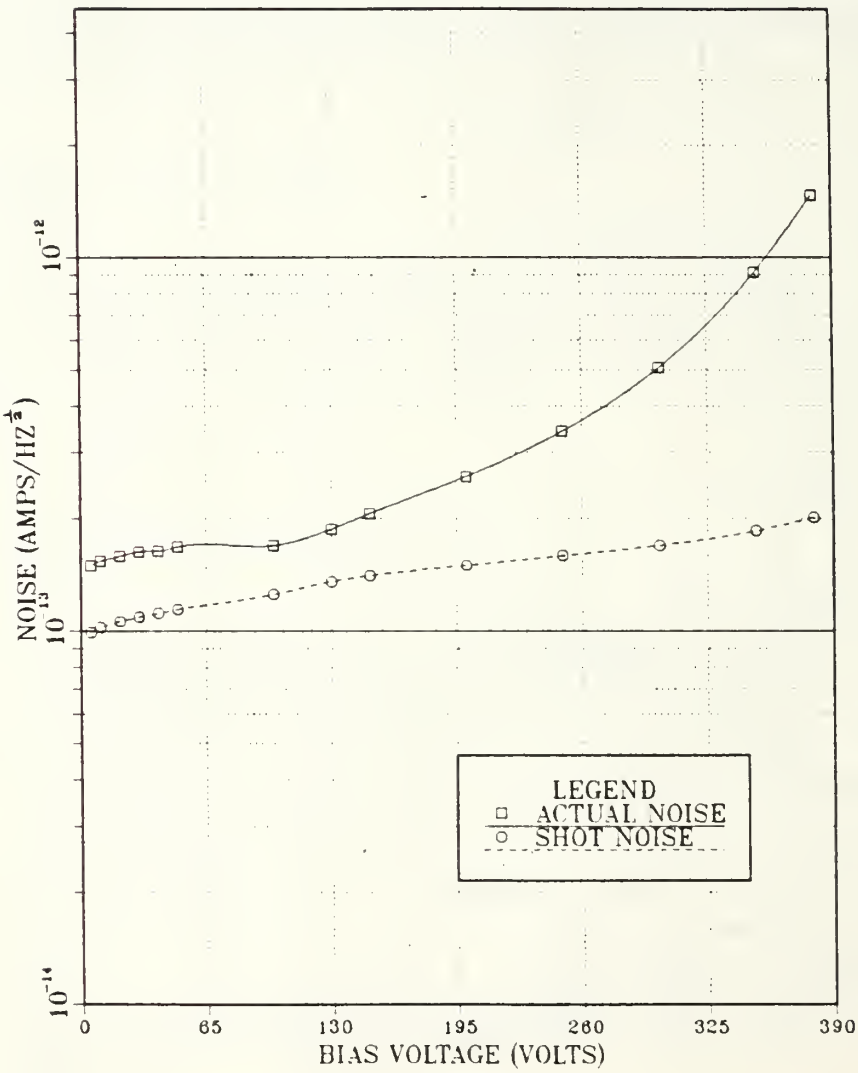

Figure 4.2 Noise versus Bias Voltage.

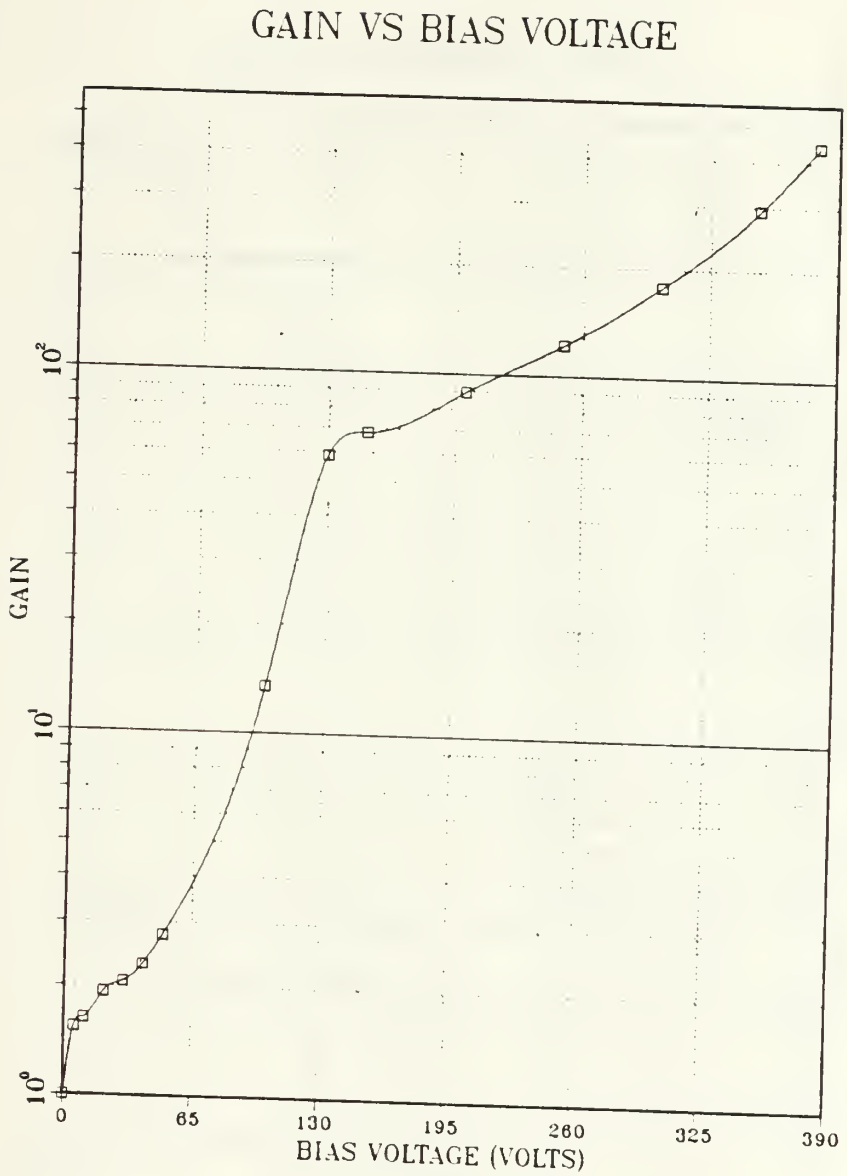

Figure 4.3 Gain versus Bias Voltage.

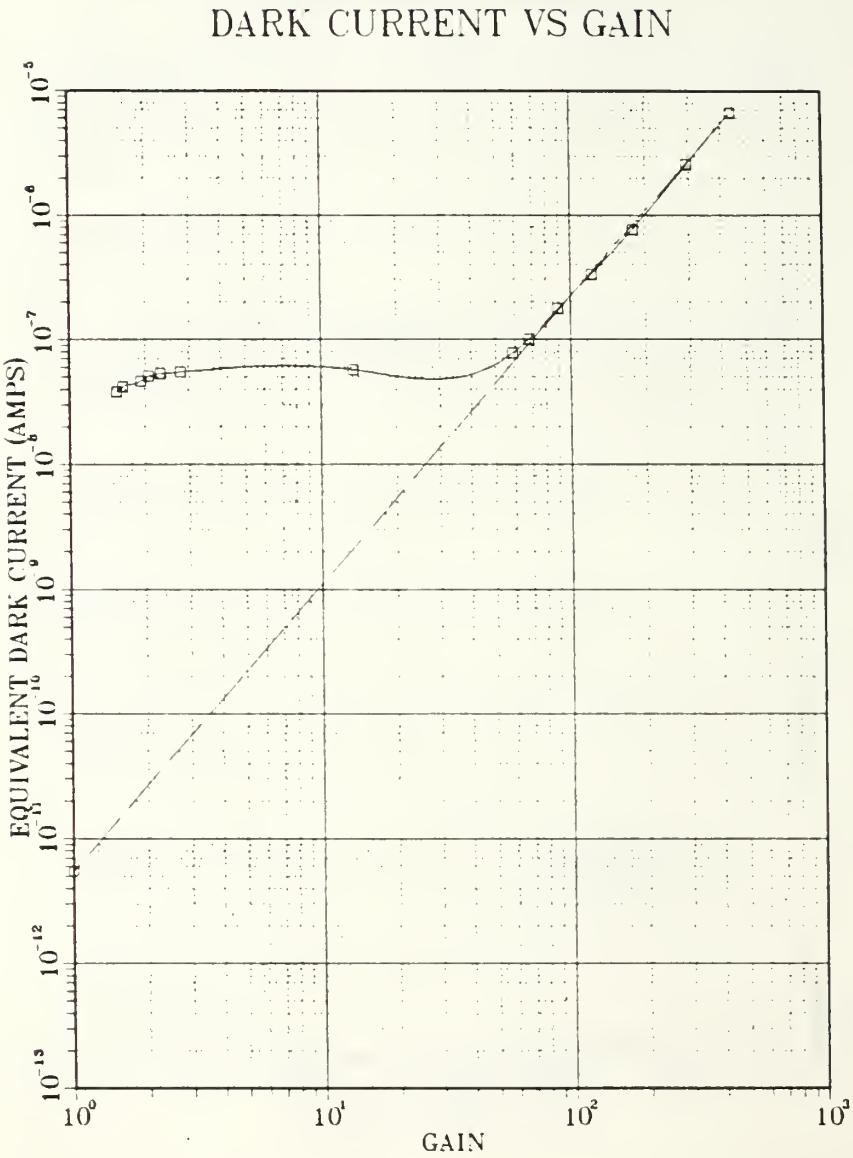

Figure 4.4 Dark Current versus Gain.

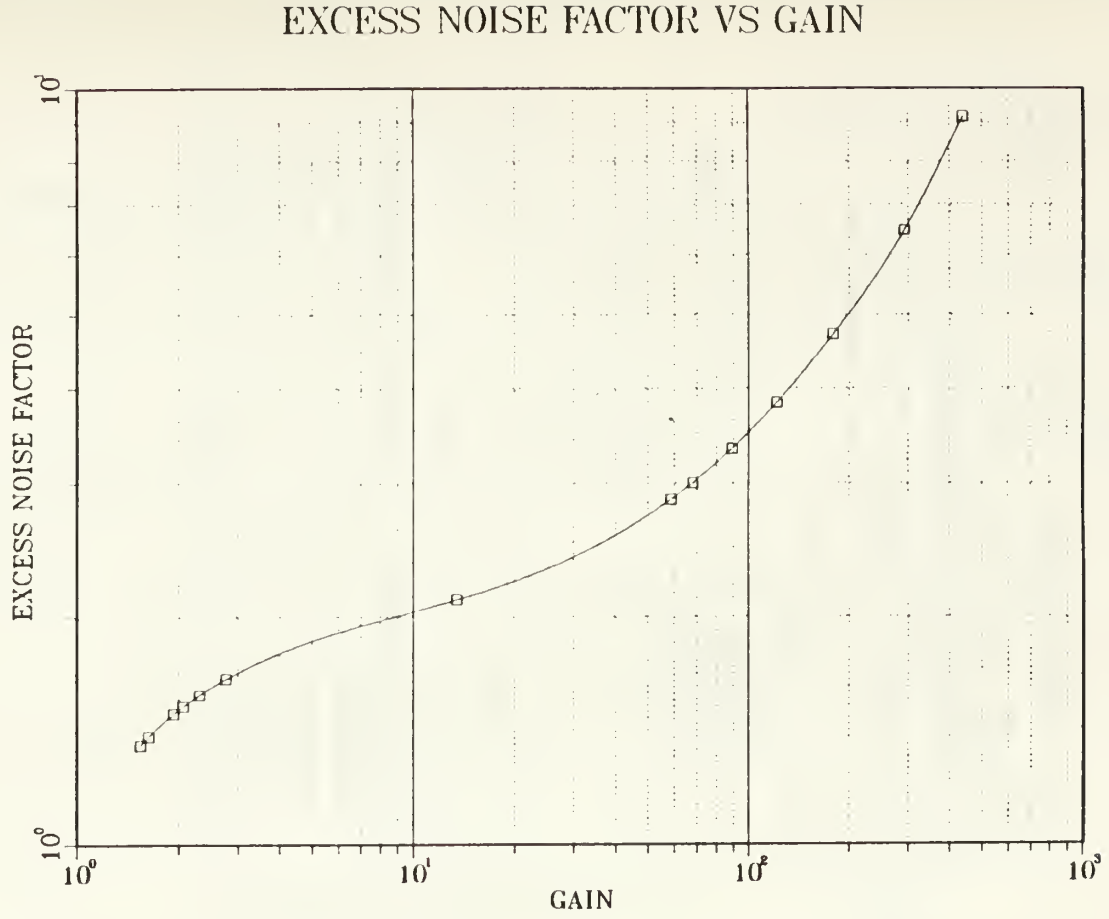

Figure 4.5 Excess Noise Factor versus Gain for K_{eff} =0.0154.

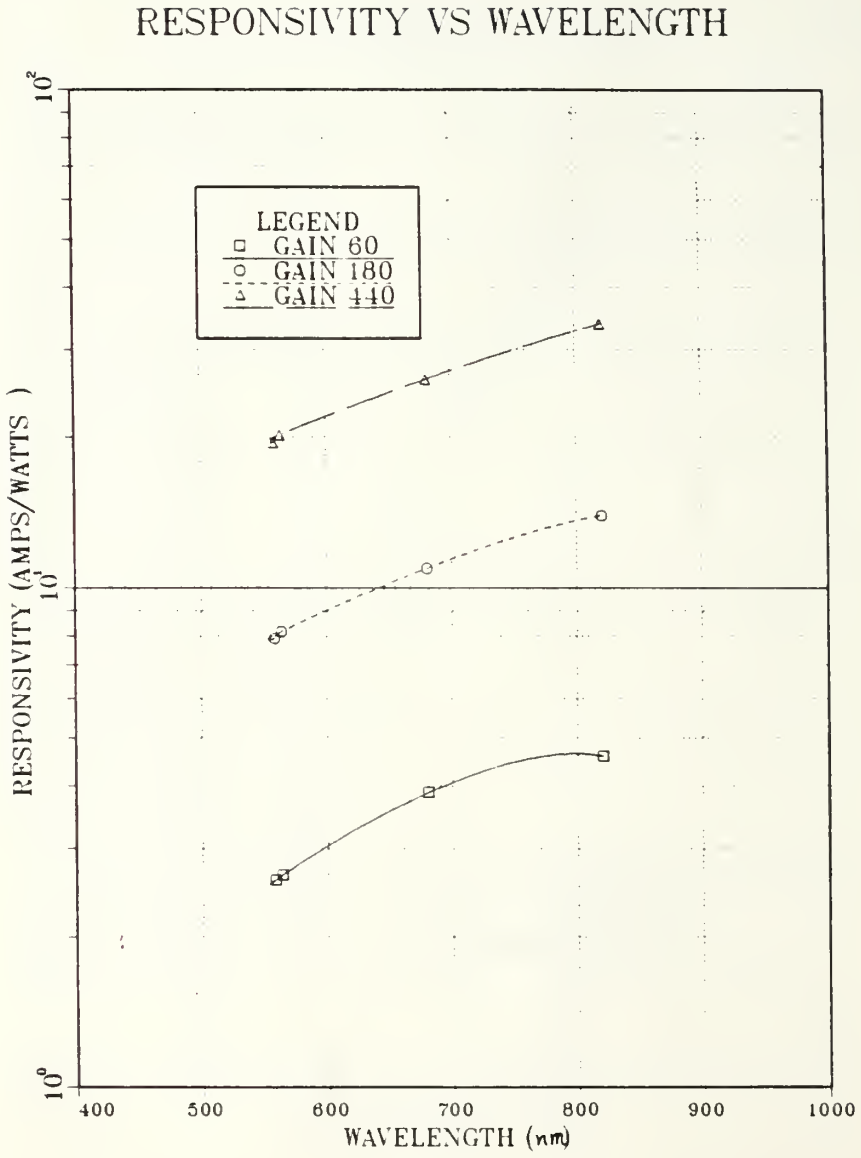

Figure 4.6 Responsivity versus Wavelength.

D. NOISE EQUIVALENT POWER (NEP)

NEP is the total optical power required for a unit signal-to noise ratio. NEP is given by [Ref. 9]

$$NEP = i_n / R\Delta f^{\frac{1}{2}} \qquad (4\text{-}1)$$

where $i_n^2 / \Delta f$ is the system noise current power spectral density given by equation (2-5). The noise current was measured directly by the HP 3561A spectrum analyzer. Figure 4.7 shows the NEP versus bias voltage as a function of wavelength. A minimum value of NEP occured around 250 volts. At higher wavelengths the NEP shifts to lower NEP powers.

E. SPECIFIC DETECTIVITY (D*)

D* is given by [Ref. 11]

$$D^* = (A\ \Delta f)^{\frac{1}{2}} / NEP, \qquad (4\text{-}2)$$

where A is the detector area, and a Δf is the electrical bandwidth. D* is a useful parameter for comparing different detectors. The larger D* the better the detector. The relation between D* and bias voltage is shown in Figure 4.8. As evident from the figure, the highest specific detectivity occures at a bias voltage of 250 volts. Figure 4.9 shows D* versus wavelength at a bias voltage 250 volts. The longer wavelengths have higher specific detectivities.

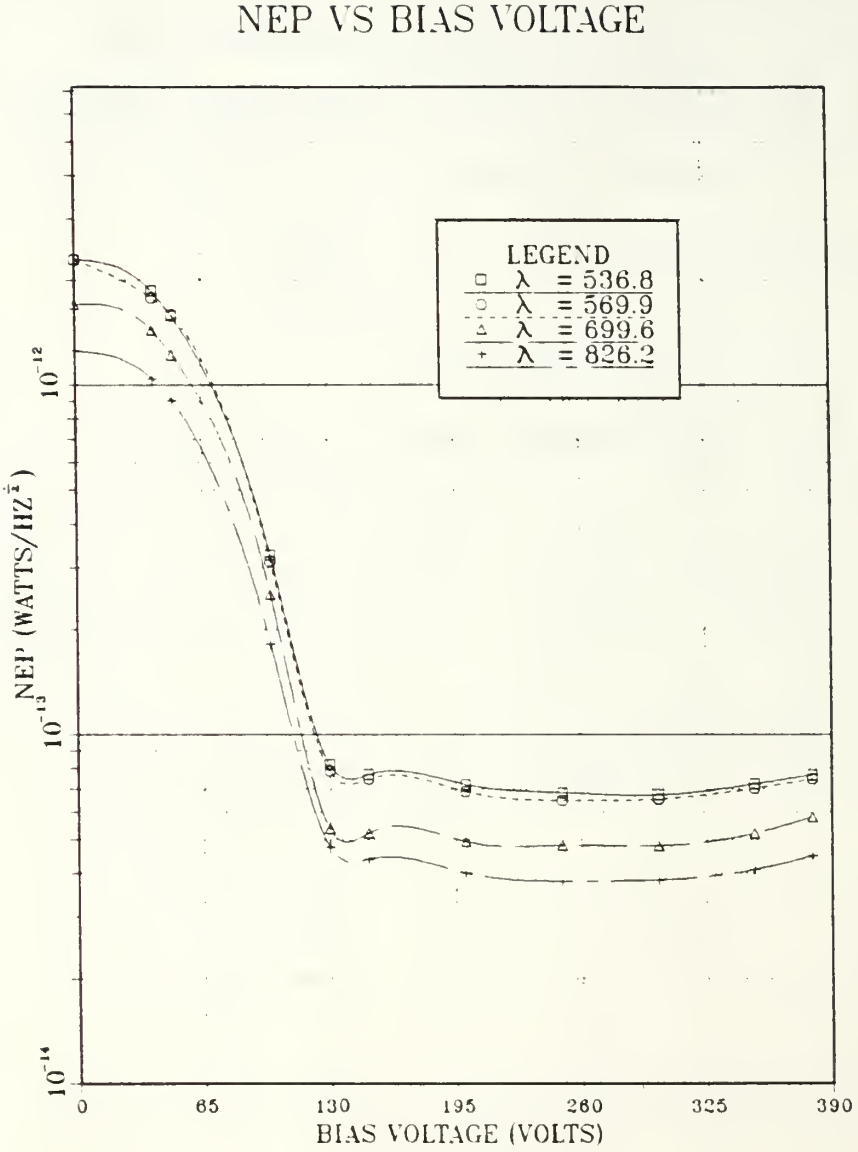

Figure 4.7 NEP versus Bias Voltage.

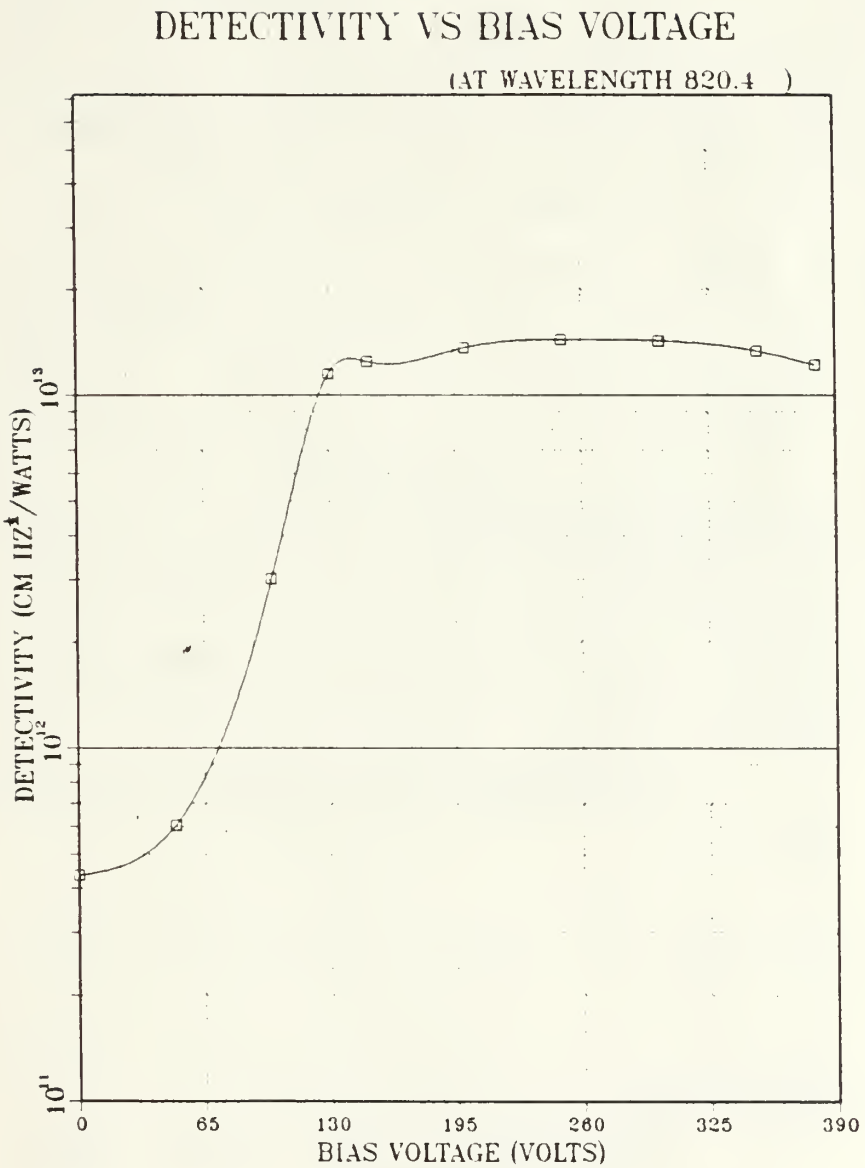

Figure 4.8 Detectivity versus Bias Voltage.

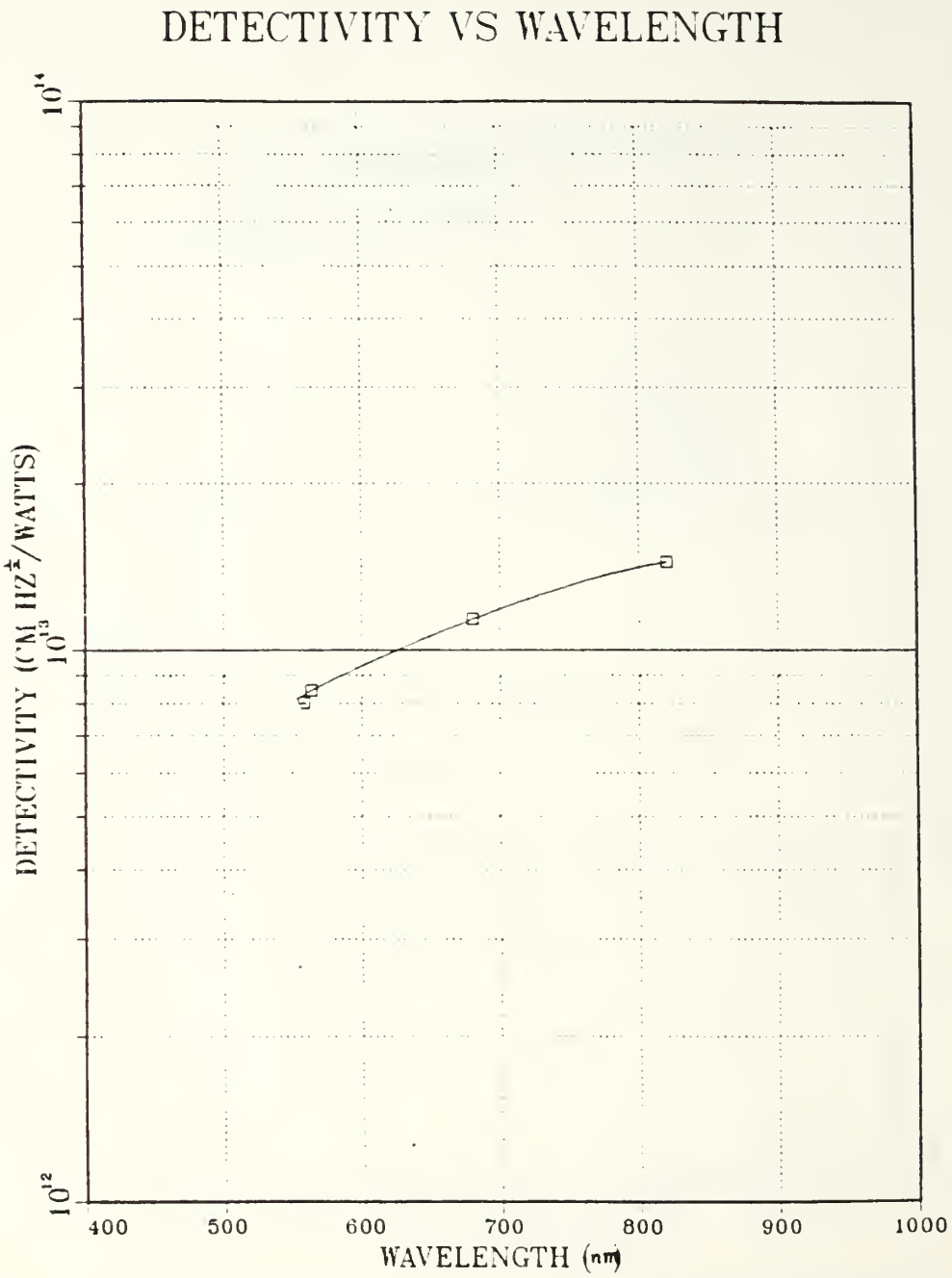

Figure 4.9 Detectivity versus Wavelength.

V. CONCLUSIONS

The noise properties of a RCA Si-RAPD were investigated at four wavelengths 563.8 nm, 569.9 nm, 699.6 nm, and 826.2 nm with modulated LEDs as light sources. An abrupt onset of gain occured at bias voltages between 120 volts and 130 volts where reach-through was established. The excess noise factor calculated at a gain a 60 for a RCA C30872 Si-RAPD is about 2.85. The C30872 Si-RAPD has a very small NEP of 3.8×10^{-14} watts/$(Hz)^{\frac{1}{2}}$ at the optimum reverse bias voltage of 250 volts which corresponds to a detectivity of 1.44×10^{13} cm $(Hz)^{\frac{1}{2}}$/watts. Since this particular RCA Si-RAPD reached its optimum detectivity at 64 % of the breakdown voltage, it would be useful to determine if this ratio is a general characteristic shared by similar Si-RAPDs.

In addition, it would be interesting to measure the noise characteristics as a funtion of the Si-RAPD temperature. At lower temperatures the pn junction reverse leakage current decreases exponentially, reducing the shot noise. It is not clear how the excess noise and the pn edge surface currents will change with temperature.

LIST OF REFERENCES

1. Heinz W. R., "An Optimized Avalanche Photodiode", IEEE Transactions on Electronic Devices, vol. ED-14, No. 5: p.239; May 1967

2. Riesz. R. P., "High Speed Semiconductor Photodiodes", Review of Scientific Instruments, p.994; Sept.1962

3. Anderson. L. K., "Microwave Photodiodes Exhibiting Microplasma-free Carrier Multiplication", Review of Scientific Instruments, p.994; Sept.1962

4. Johnson, K. M., "Photodiode Signal Enhancement Effect at Avalanche Breakdown Voltage", IEEE Transactions on Electronic Devices, p. 55; Feb., 1965

5. Verdeyen. J. T., Laser Electronics, 2nd, Prentice-Hall, 1981

6. Mcintyre, J. P., "The Distribution in Gains in Uniformly Multiplying Avalanche Photodiodes", IEEE Transactions on Electronic Devices, vol ED-19 pp. 703-713; 1972

7. Mcintyre, J. P., "Multiplication Noise in Uniform Avalanche Diodes", IEEE Transactions on Electronic Devices, vol ED-13 pp. 164-168; 1966

8. Lee, C. A., "Ionization Rates of Holes and Electrons in Silicon", Phycal Review, vol. 134, pp. A761; 1964

9. Mcintyre, J. P., "Properties of the Avalanche Phodiodes", RCA, pp. 258-278; Sep. 1974

10. Kreyszig, E., Advanced Engineering Mathmatics, 2nd, John Willy and Sons, p. 36; 1968

11. Wolfe, W. L., The Infrared Handbook, IRIA Environment Research Institute of Michigan, p. 11-40; 1978

INITIAL DISTRIBUTION LIST

		No. Copies
1.	Defense Technical Information Center Cameron Station Alexandria Va 22314	2
2.	Chairman, Code 61 Department of Physics Naval Postgraduate School Monterey, Ca 93943	1
3.	Library, Code 0142 Naval Postgraduate School Monterey Ca 93943	2
4.	Professor D.L Walters Code 61We Department of Physics Naval Postgraduate School Monterey, Ca 93943	2
5.	Professor E.A. Milne Code 61Mn Department of Physics Naval Postgraduate School Monterey, Ca 93943	2
6.	Park, Sangyul 27 tong 2 ban, 1049-761, Jang-an 1 dong, Dong-dae-moon ku, Seoul, Korea	2

Thesis
K41453
c.1

Kim

Noise characteristics of an avalanche photodiode.